



## Stability analysis for Nabla discrete fractional-order of Glucose–Insulin Regulatory System on diabetes mellitus with Mittag-Leffler kernel

G. Narayanan<sup>a,b</sup>, M. Syed Ali<sup>a</sup>, Grienggrai Rajchakit<sup>c,\*</sup>, Anuwat Jirawattanapanit<sup>d</sup>, Bandana Priya<sup>e</sup>

<sup>a</sup> Complex Systems and Networked Science Laboratory, Department of Mathematics, Thiruvalluvar University, Vellore 632 115, Tamilnadu, India

<sup>b</sup> Center for Nonlinear Systems, Chennai Institute of Technology, Chennai 600069, India

<sup>c</sup> Department of Mathematics, Faculty of Science, Maejo University, Chiang Mai 50290, Thailand

<sup>d</sup> Department of Mathematics, Faculty of Science, Phuket Rajabhat University (PKRU), 6 Thepkasatree Road, Raddasa, Phuket 83000, Thailand

<sup>e</sup> G L Bajaj Institute of Technology and Management, Greater Noida, Uttar Pradesh, India

### ARTICLE INFO

#### Keywords:

Diabetes mellitus

Fractional Nabla difference

Atangana Baleanu–Caputo derivative

Mittag-Leffler function

### ABSTRACT

In this paper, we study an existence theory as well as stability results to the new fractional Nabla difference biological model of glucose–insulin regulatory system (GIRS) on diabetes mellitus involving the Atangana Baleanu–Caputo (ABC) derivative. We consider the proposed model under ABC derivative, and it has the nonsingular Mittag-Leffler function as its kernel. We utilize the fixed point technique for the existence and uniqueness analysis. The stability of the concerned solution in Hyers–Ulam sense is also investigated. Further to derive the approximate solution in the form of series to the considered model, we use iterative technique method. Numerical simulations are given to support the theoretical results. The results show that order of the fractional derivative has a significant effect on the dynamic process. Many informations on the dynamics of GIRS in diabetes mellitus were obtained using this model. It is recognized as a deterministic fractional Nabla difference model for diabetes mellitus that provides a better control approach at fractional values for the development of an artificial pancreas.

### 1. Introduction

Diabetes mellitus (DM) is a worldwide epidemic disease characterized by plasma glucose concentrations that are mostly above normal due to an absolute or relative lack of insulin. Insulin, which is produced by the pancreas, is the most significant element in the regulation of blood glucose levels in the body. In general, the DM is caused by an insufficiency of insulin relative to the requirement of tissues. Diabetes is the most common disease that affects millions of people worldwide. Billions of dollars are spent on its treatment each year. The International Diabetes Federation (IDF) Diabetes Atlas, that approximately 415 million people in the world are living with the disease and studies also indicate that the number of diabetic patients worldwide may increase to 629 million by year 2045 [1]. The IDF had recently given the information to the effect that the top five countries in the world have the highest numbers of diabetes patients (see Fig. 1). It is a very serious problem of the world. This bleak scenario has provided numerous researchers to investigate new methods and ways to improve diabetes therapy. DM is a disease of the GIRS [2] also known as hyperglycemia (see Fig. 2 for plasma glucose–insulin interaction loops). Diabetes is a

prevalent long-term disease of the GIRS that can be classified into two types: 1 and 2. The cause of type-1 diabetes differs from that of type-2. The first is caused by a failure to produce insulin due to the lack or incorrect functionality of  $\beta$ -cells, while the second is defined by insulin resistance in the human body. Although much less severe than type-1 DM, type-2 DM accounts for 85% – 95% of all diabetes cases, having a significant impact on worldwide National Health Systems, since an untimely control of hyperglycemia facilitates the emergence of many and diverse diabetic complications such as nephropathy, neuropathy, retinopathy and etc., in both type-1 DM and type-2 DM. In type-1 DM, the individual has to measure their blood glucose levels and inject exogenous insulin with a pump several times a day. A device that does this automatically is called an artificial pancreas (AP) and would greatly improve the life of a type-1 DM. The AP is a related technologies that includes control systems, actuators, and sensors to provide a suggested plasma glucose control therapy (see Fig. 3). Many results for type-1 diabetes, i.e. diabetic patients with no pancreatic endogenous insulin release, are given in the AP literature (see [3–6]).

\* Corresponding author.

E-mail address: [syedgru@gmail.com](mailto:syedgru@gmail.com) (M. Syed Ali).

2021			2045		
Rank	Country or territory	Number of people with diabetes (millions)	Rank	Country or territory	Number of people with diabetes (millions)
1	China	140.9	1	China	174.4
2	India	74.2	2	India	124.9
3	Pakistan	33.0	3	Pakistan	62.2
4	United States of America	32.2	4	United States of America	36.3
5	Indonesia	19.5	5	Indonesia	28.6
6	Brazil	15.7	6	Brazil	23.2
7	Mexico	14.1	7	Bangladesh	22.3
8	Bangladesh	13.1	8	Mexico	21.2
9	Japan	11.0	9	Egypt	20.0
10	Egypt	10.9	10	Turkey	13.4

Fig. 1. Top 10 countries (or) territories for number of adults (20–79 years) with diabetes in 2021 and 2045.

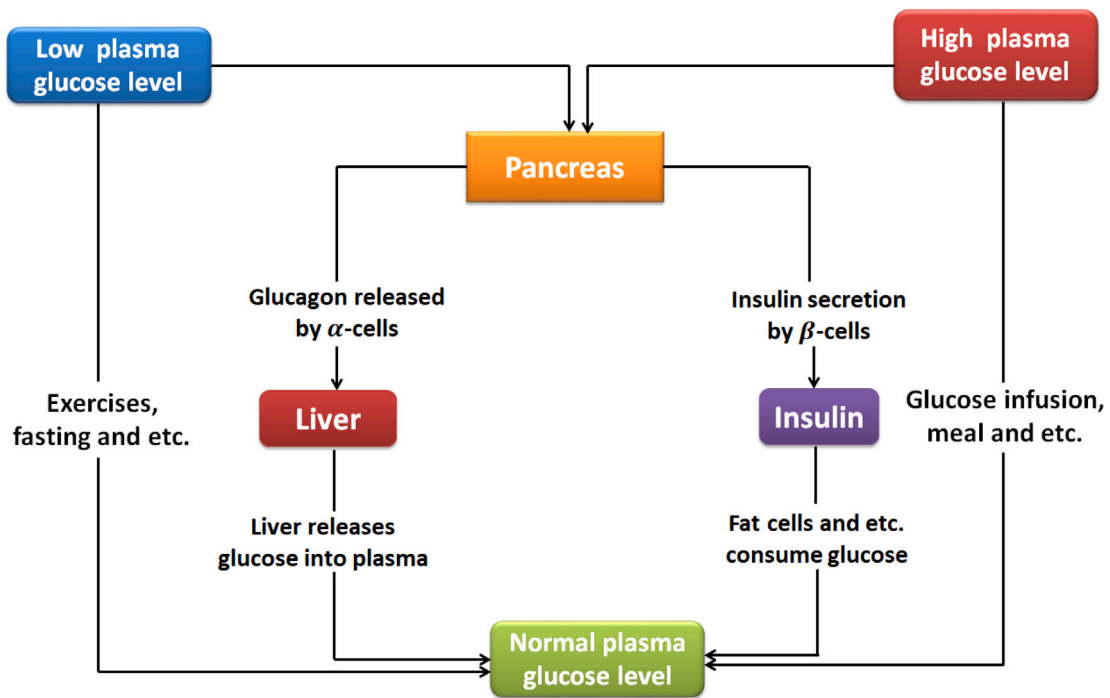


Fig. 2. Plasma glucose–insulin interaction loops.

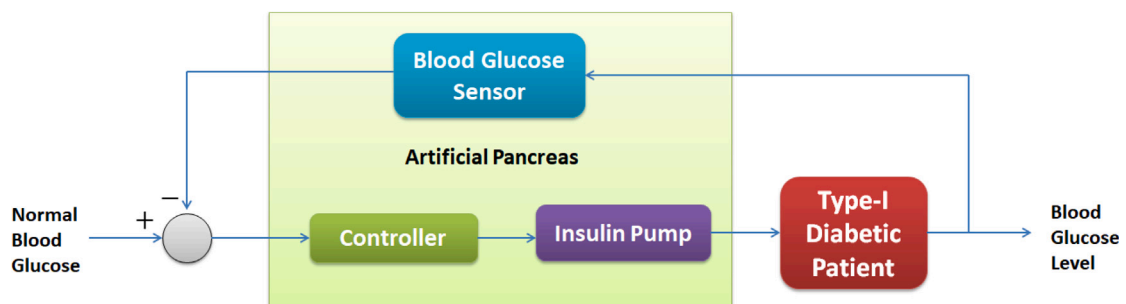


Fig. 3. The block diagram of the closed-loop system including the glucose–insulin model.

In view of that, mathematical models are valuable tools for diabetes prevention and treatment programs, and obtaining an exact solution with a good interpretation is critical. Developing bilateral interplay mathematical models of glucose–insulin from experimental research has also played a significant role in expanding the researchers vision and saving time and money. Previous estimates of current and future diabetes prevalence have been published [7–9]. Mathematical modeling has proven to be a valuable tool for better understanding disease dynamics, predicting disease outbreaks and assessing prevention or intervention efforts [10,11]. Recently, many researchers have contributed valuable information about blood sugar modeling, diabetes modeling and so on. In their mathematical model of GIRS on DM, Mahata et al. [12] constructed a fuzzy and crisp environment. The glucose dynamics in the whole body for bursting electrical activity in pancreatic  $\beta$ -cells were discussed by Han et al. [13] and numerical simulations for the GIRS were obtained. Yang et al. [14] have developed glucose infusion modeling rates and insulin injections to obtain numerical simulations for GIRS on DM recovered infected populations. These new aspects emphasize the importance of developing more effective technologies to address the blood glucose regulation problem in diabetes.

In the domains of science and engineering, differential equations can be utilized to real-world problems [15–20]. The advantages and importance of fractional-order modeling are numerous. Two crucial features of fractional derivatives are the generalization of the model and its memory effects [21–29]. A novel generalized Hattaf fractional (GHF) derivative with non-singular kernel which includes many fractional derivatives such as Atangana–Baleanu (AB) and Caputo–Fabrizio (CF) (see [30,31]). Some authors recently introduced new non-local derivatives with non-singular kernels, which have been successfully applied to some real-world problems [32,33]. To understand the dynamics of these pandemic diseases, fractional calculus play a vital role in the field of biological sciences and numbers of diseases have been modeled such as Covid-19, dengue fever, HIV and measles epidemic [34–38]. The importance of dealing with fractional-order derivatives is the involvement of memory and hereditary properties that gives a more realistic way to diabetes model. In order to explore the transmission dynamics of glucose–insulin for diabetes, researchers have developed fractional derivative mathematical models in recent years [39]. In [40], the fractional modeling of DM via Liouville–Caputo and ABC fractional derivatives is analyzed. Global dynamics of a diabetic patients with impulsive insulin injections model for CF fractional derivative were investigated in [41]. Therefore, it is of great significance to carry out research on the dynamic behavior of DM in fractional modeling, which has inspired a great deal of interest.

However, in real-world applications, the memory feature of fractional derivatives or non-locality can easily lead to numerical errors or the loss of critical information in the original systems. Some highly accurate numerical approaches were established. In practice, it remains unavailable for long-term modeling or control. This is also one of the reasons why there are fewer results in discrete time control and other discrete concerns in fractional calculus. The application of discrete fractional calculus to introduced memory effects is a novel technique [42–44]. For  $\gamma \in \mathbb{R}$ , the domain is a discrete set of values such as  $\mathbb{N}_\gamma = \{\gamma, \gamma + 1, \gamma + 2, \dots\}$ . Therefore, the discrete fractional difference systems are an important topic with promising applications in fields such as biology, medical science, economics and so on (see [45, 46]). Following that, the significant results for fractional difference equations, which are the discrete analogues of fractional differential equations is reported [47–49]. The discrete versions of new types of fractional operators involving non-singular kernels, as well as some of their features are examined [50–52], adding a new insight to discrete fractional calculus. Abdeljawad and Baleanu investigated the newly defined Nabla fractional difference operator ABC, also known as the Mittag-Leffler function in fractional discrete calculus [53]. Therefore, if these new Nabla fractional difference operators are to be used to

represent the dynamics of biological systems, discovering their discrete counterparts is critical. Until now, there is no reported the GIRS in type-1 DM patients with Nabla discrete ABC fractional-order. Even so, the discrete fractional calculus of DM model is still in its primitive stage.

In this paper, according to dynamical analysis, in which mathematical models of glucose–insulin. We present a modified DM model involves the Nabla discrete ABC fractional-order derivative gives more appropriate and comfortable behavior in a system for closed-loop design which helps to develop the AP. By the use of Nabla discrete ABC fractional-order derivative, the modified DM model permits from the incorporation of memory effects.

## 2. Methods

We recall some of the fundamental definitions of discrete fractional calculus in this section. Recently, several new definitions of Nabla fractional difference from derivatives with and without non-singular kernel [50–53]. In this paper, we generalize the model (3) involving Nabla discrete ABC fractional derivative. In this study, we aimed to derive the existence, uniqueness, and Hyers–Ulam stability results for the model based on the results discussed above and existing literature (3).

### 2.1. Background of discrete fractional calculus

**Definition 2.1** ([49]). We define the gamma function  $\Gamma(\xi)$  by the integral

$$\Gamma(\xi) = \int_0^\infty e^{-\kappa} \kappa^{\xi-1} d\kappa.$$

**Definition 2.2** ([53]). The backward difference operator is defined as follows  $\nabla \zeta(\kappa) = \zeta(\kappa) - \zeta(\kappa - 1)$  and the iteratively operator is  $\nabla^\lambda \zeta(\kappa) = \nabla(\nabla^{\lambda-1} \zeta(\kappa))$ ,  $\kappa \in \mathbb{N}_1$ .

(i) The  $m$  ascending function of  $t$  for a natural number  $m$  is

$$t^{\bar{m}} = t(t+1)(t+2), \dots, (t+m-1), \quad t \in \mathbb{R}$$

and  $t^{\bar{0}} = 1$ , where  $t^{\bar{m}}$  to  $m$  rising.

(ii) Let  $\lambda \in \mathbb{R}$ , then

$$\kappa^{\bar{\lambda}} = \frac{\Gamma(\kappa + \lambda)}{\Gamma(\kappa)},$$

where  $\kappa \in \mathbb{R} \setminus \{\dots, -2, -1, 0\}$ ,  $0^{\bar{\lambda}} = 0$ .

**Definition 2.3** (see [45,50,53]). Let  $\rho(\kappa) = \kappa - 1$  denote the backward jump operator. Then, for a function  $\phi : \mathbb{N}_\gamma = \{\gamma, \gamma + 1, \gamma + 2, \dots\} \rightarrow \mathbb{R}$ , the Nabla left fractional sum is written as

$$\nabla_\gamma^{-\lambda} \phi(\kappa) = \frac{1}{\Gamma(\lambda)} \sum_{\xi=\gamma+1}^{\kappa} (\kappa - \rho(\xi))^{\bar{\lambda}-1} \phi(\xi), \quad \kappa \in \mathbb{N}_{\gamma+1}. \tag{1}$$

**Definition 2.4** ([53]). For  $\hat{\mu} \in \mathbb{R}$ ,  $|\hat{\mu}| < 1$ , and  $\lambda, \hat{\xi}, \hat{\rho} \in \mathbb{C}$  with  $\text{Re}(\lambda) > 0$  with two parameters, the Nabla discrete Mittag-Leffler function is defined as

$$\mathbb{E}_{\lambda, \hat{\rho}}^{\hat{\xi}}(\hat{\mu}, \hat{\xi}) = \sum_{h=0}^{\infty} \hat{\mu}^h \frac{\hat{\xi}^{\bar{h}\lambda + \hat{\rho} - 1}}{\Gamma(\lambda h + \hat{\rho})}. \tag{2}$$

**Definition 2.5** (see [45,50,53]). For  $\lambda \in (0, 1)$  and a function  $\phi$ , the Atangana and Baleanu Nabla discrete new (Caputo) fractional difference is

$$\begin{aligned} {}_Y^{ABC} \nabla^\lambda \phi(\kappa) &= \frac{\mathcal{M}(\lambda)}{1-\lambda} \sum_{\xi=\gamma+1}^{\kappa} \nabla_\xi \phi(\xi) \mathbb{E}_{\bar{\lambda}}\left(\frac{-\lambda}{1-\lambda}, \kappa - \rho(\xi)\right) \\ &= \frac{\mathcal{M}(\lambda)}{1-\lambda} [\nabla \phi(\kappa) * \mathbb{E}_{\bar{\lambda}}\left(\frac{-\lambda}{1-\lambda}, \kappa\right)], \quad \lambda \in (0, \frac{1}{2}). \end{aligned}$$

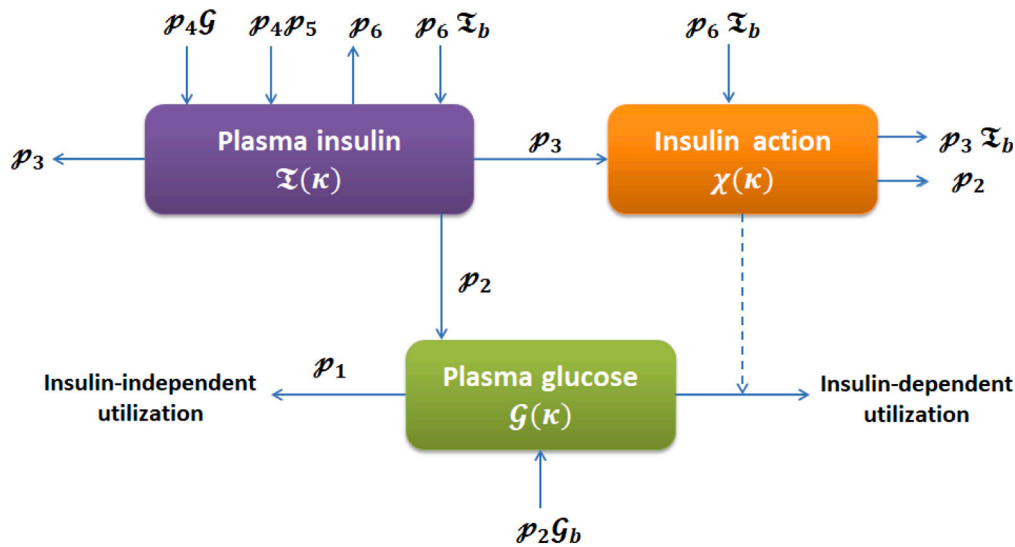


Fig. 4. Flow chart for the model (3).

The Atangana and Baleanu Nabla discrete new (Riemann–Liouville) fractional difference is

$$\begin{aligned} {}^{\text{ABR}}\nabla^{\lambda}\phi(\kappa) &= \frac{\mathcal{M}(\lambda)}{1-\lambda} \nabla_{\xi} \sum_{\xi=\gamma+1}^{\kappa} \phi(\xi) \mathbb{E}_{\lambda} \left( \frac{-\lambda}{1-\lambda}, \kappa - \rho(\xi) \right) \\ &= \frac{\mathcal{M}(\lambda)}{1-\lambda} \nabla_{\xi} [\nabla\phi(\kappa) * \mathbb{E}_{\lambda} \left( \frac{-\lambda}{1-\lambda}, \kappa \right)], \quad \lambda \in (0, \frac{1}{2}), \end{aligned}$$

where  $\mathcal{M}(\lambda)$  is a normalization constant with  $\mathcal{M}(0) = \mathcal{M}(1) = 1$ .

**Definition 2.6** ([50]). The fractional sum associated to  ${}^{\text{ABR}}\nabla^{\lambda}\phi(\kappa)$  is defined as by

$${}^{\text{AB}}\nabla^{-\lambda}\phi(\kappa) = \frac{1-\lambda}{\mathcal{M}(\lambda)}\phi(\kappa) + \frac{\lambda}{\mathcal{M}(\lambda)}\nabla_{\gamma}^{-\lambda}\phi(\kappa),$$

where  $0 < \lambda < 1$ .

### 2.2. Model description

Several biological phenomena have been extensively addressed in recent years utilizing the theory of fractional-order discrete systems; the system that consists of finite fractional-order difference equations [45]. Specifically, the fractional-order discrete systems are used, along with their associated digital data, to approximation the corresponding fractional-order differential equations. Among all mathematical models proposed for describing the behavior of the GIRS, Bergman minimal model (BMM) which shows the blood glucose concentration level of diabetic patients with continuous-time nonlinear dynamic representation (see [40,41]), is very common. In this paper, we consider BMM for modeling the GIRS in type-1 DM patients with nabla discrete ABC fractional-order, the use of the AP system as shown in Fig. 3 and the model structure as well as visualization of how the three states interact with each other have been depicted in Fig. 4.

The equations model are given by

$$\begin{cases} {}^{\text{ABC}}\nabla^{\lambda}\mathcal{G}(\kappa) = -\wp_1\mathcal{G} + \wp_2\mathcal{I} + \wp_1\mathcal{G}_b, \\ {}^{\text{ABC}}\nabla^{\lambda}\mathcal{X}(\kappa) = -\wp_2\mathcal{X} + \wp_3\mathcal{I} - \wp_3\mathcal{I}_b + \wp_6\mathcal{I}_b, \\ {}^{\text{ABC}}\nabla^{\lambda}\mathcal{I}(\kappa) = -\wp_3\mathcal{I} + \wp_4\mathcal{G} + \wp_4\wp_5 - \wp_6\mathcal{I} + \wp_6\mathcal{I}_b, \end{cases} \quad (3)$$

where  ${}^{\text{ABC}}\nabla^{\lambda}$  denotes the nabla discrete ABC fractional-order with order  $\lambda$  ( $0 < \lambda < 1$ );  $\mathcal{G}(\kappa)$  is the plasma glucose concentration;  $\mathcal{X}(\kappa)$  is the insulin effect on glucose concentration reduction;  $\mathcal{I}(\kappa)$  is the insulin concentration in plasma;  $\mathcal{G}_b$  is the basal pre injection value of

plasma glucose (mg/dl);  $\mathcal{I}_b$  is the basal pre injection value of plasma insulin ( $\mu\text{U/ml}$ );  $\wp_1$  is the insulin independent rate constant of glucose rate uptake in muscles, liver and adipose tissue ( $\text{min}^{-1}$ );  $\wp_2$  is the rate of decrease in tissue glucose uptake ability ( $\text{min}^{-1}$ );  $\wp_3$  is the insulin independent increase in glucose uptake ability in tissue per unit of insulin concentration  $\mathcal{I}_b$  ( $\text{min}^{-2} (\mu\text{U/ml})$ );  $\wp_4$  is the rate of the pancreatic  $\beta$ -cells release of insulin after the glucose injection and with glucose concentration above ( $\text{h}((\mu\text{U/ml})\text{min}^{-2}(\text{mg/dl})^{-1})$ );  $\wp_5$  is the threshold value of glucose above which the pancreatic  $\beta$ -cells release insulin (mg/dl);  $\wp_6$  is the decay rate for insulin in plasma ( $\text{min}^{-1}$ ) pancreatic  $\beta$ -cells release insulin ( $\text{min}^{-1}$ ).

To accomplish this, we write the right hand sides of (3) as

$$\begin{cases} \theta_1(\kappa, \mathcal{G}, \mathcal{X}, \mathcal{I}) = -\wp_1\mathcal{G} + \wp_2\mathcal{I} + \wp_1\mathcal{G}_b, \\ \theta_2(\kappa, \mathcal{G}, \mathcal{X}, \mathcal{I}) = -\wp_2\mathcal{X} + \wp_3\mathcal{I} - \wp_3\mathcal{I}_b + \wp_6\mathcal{I}_b, \\ \theta_3(\kappa, \mathcal{G}, \mathcal{X}, \mathcal{I}) = -\wp_3\mathcal{I} + \wp_4\mathcal{G} + \wp_4\wp_5 - \wp_6\mathcal{I} + \wp_6\mathcal{I}_b, \end{cases} \quad (4)$$

and with initial conditions

$$\mathcal{G}(\gamma) = \mathcal{G}_{\gamma}, \mathcal{X}(\gamma) = \mathcal{X}_{\gamma}, \mathcal{I}(\gamma) = \mathcal{I}_{\gamma}.$$

Further we use

$$\mathfrak{S}(\kappa) = \begin{cases} \mathcal{G}(\kappa) \\ \mathcal{X}(\kappa) \\ \mathcal{I}(\kappa) \end{cases}, \quad \mathfrak{S}(\gamma) = \begin{cases} \mathcal{G}(\gamma) \\ \mathcal{X}(\gamma) \\ \mathcal{I}(\gamma) \end{cases}, \quad \Theta(\kappa, \mathfrak{S}(t)) = \begin{cases} \theta_1(\kappa, \mathcal{G}, \mathcal{X}, \mathcal{I}) \\ \theta_2(\kappa, \mathcal{G}, \mathcal{X}, \mathcal{I}) \\ \theta_3(\kappa, \mathcal{G}, \mathcal{X}, \mathcal{I}) \end{cases} \quad (5)$$

and

$$\Theta_{\gamma} = \begin{cases} \theta_1(\gamma, \mathcal{G}(\gamma), \mathcal{X}(\gamma), \mathcal{I}(\gamma)) \\ \theta_2(\gamma, \mathcal{G}(\gamma), \mathcal{X}(\gamma), \mathcal{I}(\gamma)) \\ \theta_3(\gamma, \mathcal{G}(\gamma), \mathcal{X}(\gamma), \mathcal{I}(\gamma)) \end{cases} \quad (6)$$

Eqs. (3) and (6), it is possible to write

$${}^{\text{ABC}}\nabla_{\gamma}^{\lambda}\mathfrak{S}(\kappa) = \Theta(\kappa, \mathfrak{S}(\kappa)), \quad \kappa \in \mathbb{N}_{\gamma}. \quad (7)$$

By applying AB fractional integral in the solution of system (7), and it follows from Definition 2.6 that

$$\mathfrak{S}(\kappa) = \mathfrak{S}(\gamma) + \frac{1-\lambda}{\mathcal{M}(\lambda)}\Theta(\kappa, \mathfrak{S}(\kappa)) + \frac{\lambda}{\mathcal{M}(\lambda)\Gamma(\lambda)} \sum_{\xi=\gamma+1}^{\kappa} (\kappa - \rho(\xi))^{\lambda-1} \Theta(\xi, \mathfrak{S}(\xi)). \quad (8)$$

For onward analysis, we claim the assumptions to be hold:

(A1). There exist  $\eta_\alpha > 0$ , such that

$$|\Theta(\kappa, \mathfrak{F}) - \Theta(\kappa, \widehat{\mathfrak{F}})| \leq \eta_\alpha \|\mathfrak{F} - \widehat{\mathfrak{F}}\|.$$

(A2). There exist constants  $\varphi_\alpha > 0$  and  $\psi_\alpha > 0$ , such that for any  $\mathfrak{F}, \widehat{\mathfrak{F}} \in \mathbb{R}$ , we have  $|\Theta(\kappa, \mathfrak{F})| \leq \varphi_\alpha$  and  $|\Theta(\kappa, \widehat{\mathfrak{F}})| \leq \psi_\alpha$ .

**Lemma 2.7** ([50]). If  $0 < \lambda < 1$ , we have

$${}_{\gamma}^{AB} \nabla^{-\lambda} ({}_{\gamma}^{ABC} \nabla^{\lambda} \phi(\kappa)) = \phi(\kappa) - \phi(\gamma).$$

**Lemma 2.8** (Krasnoselski Fixed Point Theorem [31]). Let  $\mathfrak{U} \subset X$  be a closed, bounded, convex non empty subset of  $X$  and there exist two operators  $\Omega$  and  $\Xi$  such that

- (1)  $\Omega$  is a contraction mapping.
- (2)  $\Omega\mathfrak{F} + \Xi\widehat{\mathfrak{F}} \in \mathfrak{U}$  whenever  $\mathfrak{F}, \widehat{\mathfrak{F}} \in \mathfrak{U}$ .
- (3)  $\Xi$  is compact and continuous.

Then there exists at least one solution  $\mathfrak{F} \in \mathfrak{U}$  such that  $\Omega\mathfrak{F} + \Xi\mathfrak{F} = \mathfrak{F}$ .

### 2.3. Existence and uniqueness of the solution

In this section, we investigate the existence and the uniqueness of the solutions of the considered model (3). Fixed point theory is a powerful tool to use to study the afore required need. Therefore, we use the fixed point theorem to determine the existence findings for at least one solution to model (3).

**Theorem 2.9.** Under the Assumption (A1) and (A2), the problem (7) has a solution if

- (i)  $\mathfrak{R} < 1$ ,
- (ii)  $\frac{\|\mathfrak{F}_\gamma\|_c + \mathcal{J}}{1 - \mathfrak{R}} \leq \beta$ ,

where  $\mathcal{J} = \frac{1-\lambda}{\mathcal{M}(\lambda)}\varphi_\alpha + \frac{1}{\mathcal{M}(\lambda)\mathbf{B}(K-\gamma,\lambda)}\psi_\alpha$ ,  $\mathfrak{R} = \left(\frac{1-\lambda}{\mathcal{M}(\lambda)} + \frac{1}{\mathcal{M}(\lambda)\mathbf{B}(K-\gamma,\lambda)}\right)\eta_\alpha$ . Consequently the considered model (3) has a solution.

**Proof.** A closed and compact set  $\mathfrak{U}$  is defined as  $\mathfrak{U} = \{\mathfrak{F} \in \mathfrak{U} : \|\mathfrak{F}\| \leq \beta\}$ .

We define two operators  $\Omega$  and  $\Xi$  as

$$\Omega\mathfrak{F}(\kappa) = \mathfrak{F}_\gamma + \frac{1-\lambda}{\mathcal{M}(\lambda)}\Theta(\kappa, \mathfrak{F}(\kappa)), \tag{9}$$

$$\Xi\mathfrak{F}(\kappa) = \frac{\lambda}{\mathcal{M}(\lambda)\Gamma(\lambda)} \sum_{\xi=\gamma+1}^{\kappa} (\kappa - \rho(\xi))^{\lambda-1} \Theta(\xi, \mathfrak{F}(\xi)). \tag{10}$$

The operator equation can be written as  $\mathfrak{F}(\kappa) = \Omega\mathfrak{F}(\kappa) + \Xi\mathfrak{F}(\kappa)$ . For  $\kappa \in (\gamma, K]$ , we provide proof in various steps as:

**Step 1:** We prove that  $\Omega$  is contraction.

For  $\mathfrak{F}(\kappa), \widehat{\mathfrak{F}}(\kappa) \in \mathfrak{U}$  and Assumption (A1), then

$$\|\Omega\mathfrak{F}(\kappa) - \Omega\widehat{\mathfrak{F}}(\kappa)\| \leq \frac{1-\lambda}{\mathcal{M}(\lambda)}\eta_\alpha \|\mathfrak{F}(\kappa) - \widehat{\mathfrak{F}}(\kappa)\|,$$

if  $\frac{1-\lambda}{\mathcal{M}(\lambda)}\eta_\alpha < 1$ . Therefore  $\Omega$  is contraction mapping.

**Step 2:** We prove  $\Omega\widehat{\mathfrak{F}}(\kappa) + \Xi\mathfrak{F}(\kappa) \in \mathfrak{U}$ , for  $\widehat{\mathfrak{F}}(\kappa), \mathfrak{F}(\kappa) \in \mathfrak{U}$ .

By using Minkowski inequality, it follows that

$$\begin{aligned} \|\Omega\widehat{\mathfrak{F}}(\kappa) + \Xi\mathfrak{F}(\kappa)\| &\leq \|\mathfrak{F}_\gamma\|_c + \sup_{\gamma < \kappa \leq K} \frac{1-\lambda}{\mathcal{M}(\lambda)} \left| \Theta(\kappa, \widehat{\mathfrak{F}}(\kappa)) - \Theta(0) \right| \\ &+ \sup_{\gamma < \kappa \leq K} \frac{\lambda}{\mathcal{M}(\lambda)\Gamma(\lambda)} \\ &\times \sum_{\xi=\gamma+1}^{\kappa} (\kappa - \rho(\xi))^{\lambda-1} \left| \Theta(\xi, \mathfrak{F}(\xi)) - \Theta(0) \right| \\ &+ \sup_{\gamma < \kappa \leq K} \frac{1-\lambda}{\mathcal{M}(\lambda)} \left| \Theta(0) \right| \\ &+ \sup_{\gamma < \kappa \leq K} \frac{\lambda}{\mathcal{M}(\lambda)\Gamma(\lambda)} \sum_{\xi=\gamma+1}^{\kappa} (\kappa - \rho(\xi))^{\lambda-1} \left| \Theta(0) \right|. \end{aligned} \tag{11}$$

By using Assumptions (A1), one has

$$\sup_{\gamma < \kappa \leq K} \frac{1-\lambda}{\mathcal{M}(\lambda)} \left| \Theta(\kappa, \widehat{\mathfrak{F}}(\kappa)) - \Theta(0) \right| \leq \frac{(1-\lambda)\eta_\alpha}{\mathcal{M}(\lambda)} \|\widehat{\mathfrak{F}}(\kappa)\| \tag{12}$$

and

$$\begin{aligned} \sup_{\gamma < \kappa \leq K} \frac{\lambda}{\mathcal{M}(\lambda)\Gamma(\lambda)} \sum_{\xi=\gamma+1}^{\kappa} (\kappa - \rho(\xi))^{\lambda-1} \left| \Theta(\xi, \mathfrak{F}(\xi)) - \Theta(0) \right| \\ \leq \frac{\lambda\eta_\alpha}{\mathcal{M}(\lambda)\Gamma(\lambda)} \sum_{\xi=\gamma+1}^{\kappa} (\kappa - \rho(\xi))^{\lambda-1} (\kappa - \gamma)^0 \|\mathfrak{F}(\kappa)\|. \end{aligned}$$

Take  $(\kappa - \gamma)^0 = 1$  and from Definition 2.3, it follows that

$$\sum_{\xi=\gamma+1}^{\kappa} (\kappa - \rho(\xi))^{\lambda-1} (\kappa - \gamma)^0 = \frac{\Gamma(\kappa - \gamma + \lambda)}{\lambda\Gamma(\kappa - \gamma)}.$$

Therefore

$$\begin{aligned} \sup_{\gamma < \kappa \leq K} \frac{\lambda}{\mathcal{M}(\lambda)\Gamma(\lambda)} \sum_{\xi=\gamma+1}^{\kappa} (\kappa - \rho(\xi))^{\lambda-1} \left| \Theta(\xi, \mathfrak{F}(\xi)) - \Theta(0) \right| \\ \leq \frac{\eta_\alpha}{\mathcal{M}(\lambda)\mathbf{B}(K - \gamma, \lambda)} \|\mathfrak{F}(\kappa)\|. \end{aligned} \tag{13}$$

Combing (11)–(13), we have

$$\begin{aligned} \|\Omega\widehat{\mathfrak{F}}(\kappa) + \Xi\mathfrak{F}(\kappa)\| &\leq \|\mathfrak{F}_\gamma\|_c + \frac{(1-\lambda)}{\mathcal{M}(\lambda)}\varphi_\alpha + \frac{1}{\mathcal{M}(\lambda)\mathbf{B}(K - \gamma, \lambda)}\psi_\alpha \\ &+ \left( \frac{(1-\lambda)\eta_\alpha}{\mathcal{M}(\lambda)} + \frac{\eta_\alpha}{\mathcal{M}(\lambda)\mathbf{B}(K - \gamma, \lambda)} \right) \beta \\ &\leq \|\mathfrak{F}_\gamma\|_c + \mathcal{J} + \mathfrak{R}\beta \leq \beta. \end{aligned}$$

**Step 3:** We prove that operator  $\Xi$  is continuous and  $\Xi(\mathfrak{U})$  is relatively compact.

For  $\mathfrak{F}(\kappa) \in \mathfrak{U}$ , taking a sequence  $\mathfrak{F}_m(\kappa)$ , whose limit  $\mathfrak{F}(\kappa)$

$$\|\Xi\mathfrak{F}_m(\kappa) - \Xi\mathfrak{F}(\kappa)\| \leq \frac{\eta_\alpha}{\mathcal{M}(\lambda)\mathbf{B}(K - \gamma, \lambda)} \|\mathfrak{F}_m(\kappa) - \mathfrak{F}(\kappa)\|. \tag{14}$$

Thus, we conclude from (14) that  $\Xi\mathfrak{F}_m(\kappa) \rightarrow \Xi\mathfrak{F}(\kappa)$  as  $\mathfrak{F}_m(\kappa) \rightarrow \mathfrak{F}(\kappa)$ , this implies that the operator  $\Xi$  is continuous.

Then, we show that  $\Xi$  is relatively compact.

For  $\mathfrak{F}(\kappa) \in \mathfrak{U}$ , we have

$$\Xi\mathfrak{F}(\kappa) = \left| \sup_{\gamma < \kappa \leq K} \frac{\lambda}{\mathcal{M}(\lambda)} \sum_{\xi=\gamma+1}^{\kappa} (\kappa - \rho(\xi))^{\lambda-1} \Theta(\xi, \mathfrak{F}(\xi)) \right| \leq \beta,$$

which means that operator  $\Xi$  is bounded.

Let  $\mathbb{N}_0 \in \mathbb{N}_\gamma$  and  $\mathbb{N}_0 < \kappa_1 < \kappa_2$ , we get from Definition 2.3 that

$$\begin{aligned} \|\Xi\mathfrak{F}(\kappa_2) - \Xi\mathfrak{F}(\kappa_1)\| &\leq \frac{\varphi_\alpha}{\mathcal{M}(\lambda)} \left( \nabla_\gamma^{-\lambda}(\kappa_2 - \gamma)^0 - \nabla_\gamma^{-\lambda}(\kappa_1 - \gamma)^0 \right) \\ &+ \nabla_{\kappa_1}^{-\lambda}(\kappa_2 - \kappa_1)^0 \\ &\leq \frac{\varphi_\alpha}{\mathcal{M}(\lambda)} \frac{((\kappa_2 - \gamma)^\lambda - (\kappa_1 - \gamma)^\lambda) + (\kappa_2 - \kappa_1)^\lambda}{\Gamma(\lambda + 1)}, \end{aligned}$$

which implies that  $\|\Xi\mathfrak{F}(\kappa_2) - \Xi\mathfrak{F}(\kappa_1)\| \rightarrow 0$  as  $\kappa_2 \rightarrow \kappa_1$ . Thus, the operator  $\Xi$  is uniformly Cauchy in  $\mathfrak{U}$ . Consequently, by Arzela–Ascoli theorem [31], is relatively compact.

**Step 4:** There exists a solution  $\mathfrak{F}(\kappa) \in \mathfrak{U}$  when  $\mathfrak{F}(\kappa) = \Omega\mathfrak{F}(\kappa) + \Xi\mathfrak{F}(\kappa)$ .

If  $\mathfrak{F}(\kappa) = \Sigma\mathfrak{F}(\kappa) = \Omega\mathfrak{F}(\kappa) + \Xi\mathfrak{F}(\kappa)$ , by using Minkowski inequality, we get

$$\begin{aligned} \|\mathfrak{F}(\kappa)\| &= \|\Omega\mathfrak{F}(\kappa) + \Xi\mathfrak{F}(\kappa)\| \leq \|\mathfrak{F}_\gamma\|_c + \frac{1-\lambda}{\mathcal{M}(\lambda)}\varphi_\alpha \\ &+ \frac{1}{\mathcal{M}(\lambda)\mathbf{B}(K - \gamma, \lambda)}\psi_\alpha \leq \beta, \end{aligned}$$

which means that  $\mathfrak{F}(\kappa) \in \mathfrak{U}$ . By the consequence of Krasnoselskii fixed point theorem, therefore, model (3) admits at least one solution.

**Theorem 2.10.** Under the continuity  $\Theta$  together with Assumption (A1) and if the condition  $\mu_\alpha < 1$ , then the problem (7) has a unique solution, where  $\mu_\alpha = \frac{1-\lambda}{\mathcal{M}(\lambda)} + \frac{1}{\mathcal{M}(\lambda)\mathbf{B}(K-\gamma,\lambda)}\eta_\alpha$ . Consequently the model (3) has unique solution.

2.4. Ulam–Hyers (U–H) and Ulam–Hyers Rassias (U–H–R) stability

Ulam suggested the stability of functional equations derived from the stability problem of group homomorphism in 1940. Hyers solves the stability problem of additive mappings over Banach spaces in 1941. Since then, U–H stability has developed rapidly. The concept of U–H type stability is very important in many realistic situations in biology. This kind of stability ensures that a close exact solution exists. Recently, U–H and U–H–R stability for fractional derivatives have been studied in many research articles (refer [31,37]).

**Definition 2.11** (see [31,37]). Let  $\mathfrak{F}(\kappa) \in X$  be any solution of  $\|\mathcal{I}_{\gamma}^{ABC} \nabla^{\lambda} \mathfrak{F}(\kappa) - \Theta(\kappa, \mathfrak{F}(\kappa))\| \leq \epsilon$ , for  $\epsilon > 0$ , then model (3) is U–H stable if there is a unique solution to model (3) with  $\mu_{\alpha} > 0$  such that

$$\|\mathfrak{F}(\kappa) - \hat{\mathfrak{F}}(\kappa)\| \leq \mu_{\alpha} \epsilon, \quad \epsilon > 0.$$

**Remark 2.12** (see [31,45]). Consider a small perturbation  $\varpi \in (\gamma, K]$  satisfy following

- (i)  $|\varpi(\kappa)| < \epsilon$ , for  $\epsilon > 0$ .
- (ii) For  $\kappa \in (\gamma, K]$ , we have the model

$$\begin{cases} \mathcal{I}_{\gamma}^{ABC} \nabla^{\lambda} \mathfrak{F}(\kappa) = \Theta(\kappa, \mathfrak{F}(\kappa)) + \varpi(\kappa), \\ \mathfrak{F}(\gamma) = \mathfrak{F}_{\gamma}. \end{cases}$$

**Lemma 2.13.** The solution of the perturbed problem

$$\begin{cases} \mathcal{I}_{\gamma}^{ABC} \nabla^{\lambda} \mathfrak{F}(\kappa) = \Theta(\kappa, \mathfrak{F}(\kappa)) + \varpi(\kappa), \\ \mathfrak{F}(\gamma) = \mathfrak{F}_{\gamma}, \end{cases} \tag{15}$$

satisfies the relation

$$\|\mathfrak{F}(\kappa) - \mathcal{Z}\mathfrak{F}(\kappa)\| \leq \left(\frac{1-\lambda}{\mathcal{M}(\lambda)} + \frac{1}{\mathcal{M}(\lambda)\mathbf{B}(K-\gamma, \lambda)}\right)\epsilon.$$

**Theorem 2.14.** Under Assumption (A1) with Lemma 2.13, the solution of problem (7) is U–H stable, if the following condition hold,

$$\frac{\left(\frac{1-\lambda}{\mathcal{M}(\lambda)} + \frac{1}{\mathcal{M}(\lambda)\mathbf{B}(K-\gamma, \lambda)}\right)}{\left[1 - \left(\frac{1-\lambda}{\mathcal{M}(\lambda)} + \frac{1}{\mathcal{M}(\lambda)\mathbf{B}(K-\gamma, \lambda)}\right)\eta_{\alpha}\right]} < 1.$$

Consequently the approximate solution of the considered model (3) is U–H stable.

**Definition 2.15** (see [31,37]). Let  $\psi(\kappa) \in \mathbb{C}[(\gamma, K], \mathbb{R})$  and  $\mathfrak{F}(\kappa) \in X$  be any solution of  $\|\mathcal{I}_{\gamma}^{ABC} \nabla^{\lambda} \mathfrak{F}(\kappa) - \Theta(\kappa, \mathfrak{F}(\kappa))\| \leq \psi(\kappa)\epsilon$ , for  $\epsilon > 0$ , then model (3) is U–H–R stable there is a unique solution to model (3) with  $\mu_{\alpha} > 0$ , such as

$$\|\mathfrak{F}(\kappa) - \hat{\mathfrak{F}}(\kappa)\| \leq \psi(\kappa)\mu_{\alpha}\epsilon, \quad \epsilon > 0.$$

**Remark 2.16** (see [37,45]). Consider a small perturbation  $\varpi \in (\gamma, K]$  with the properties

- (i)  $|\varpi(\kappa)| < \psi(\kappa)\epsilon$ , for  $\epsilon > 0$ .
- (ii) For  $\kappa \in (\gamma, K]$ , we have the following model

$$\begin{cases} \mathcal{I}_{\gamma}^{ABC} \nabla^{\lambda} \mathfrak{F}(\kappa) = \Theta(\kappa, \mathfrak{F}(\kappa)) + \varpi(\kappa), \\ \mathfrak{F}(\gamma) = \mathfrak{F}_{\gamma}. \end{cases}$$

**Lemma 2.17.** The solution of the perturbed problem

$$\begin{cases} \mathcal{I}_{\gamma}^{ABC} \nabla^{\lambda} \mathfrak{F}(\kappa) = \Theta(\kappa, \mathfrak{F}(\kappa)) + \varpi(\kappa), \\ \mathfrak{F}(\gamma) = \mathfrak{F}_{\gamma}, \end{cases} \tag{16}$$

satisfies the given relation

$$\|\mathfrak{F}(\kappa) - \mathcal{Z}\mathfrak{F}(\kappa)\| \leq \left(\frac{1-\lambda}{\mathcal{M}(\lambda)} + \frac{1}{\mathcal{M}(\lambda)\mathbf{B}(K-\gamma, \lambda)}\right)\psi(\kappa)\epsilon.$$

**Theorem 2.18.** Under Assumption (A1) with Lemma 2.17, the solution of problem (7) is U–H–R stable, if the following condition hold,

$$\frac{\left(\frac{1-\lambda}{\mathcal{M}(\lambda)} + \frac{1}{\mathcal{M}(\lambda)\mathbf{B}(K-\gamma, \lambda)}\right)}{\left[1 - \left(\frac{1-\lambda}{\mathcal{M}(\lambda)} + \frac{1}{\mathcal{M}(\lambda)\mathbf{B}(K-\gamma, \lambda)}\right)\eta_{\alpha}\right]} < 1.$$

Consequently the approximate solution of the considered model (3) is U–H–R stable.

2.5. Approximate solution of the considered model

Since the DM model with Nabla discrete ABC fractional derivative has three equations. To obtain the solution, we will use an iterative technique with the help of the Nabla discrete AB integral operator.

Now we apply Eq. (8) on the solution (3), and get the below results

$$\begin{aligned} \mathcal{G}(\kappa) &= \mathcal{G}(\gamma) + \frac{1-\lambda}{\mathcal{M}(\lambda)}\theta_1(\kappa, \mathcal{G}(\kappa), \mathcal{X}(\kappa), \mathcal{I}(\kappa)) \\ &\quad + \frac{\lambda}{\mathcal{M}(\lambda)\Gamma(\lambda)} \sum_{\xi=\gamma+1}^{\kappa} (\kappa - \rho(\xi))^{\lambda-1} \theta_1(\xi, \mathcal{G}(\xi), \mathcal{X}(\xi), \mathcal{I}(\xi)), \\ \mathcal{X}(\kappa) &= \mathcal{X}(\gamma) + \frac{1-\lambda}{\mathcal{M}(\lambda)}\theta_2(\kappa, \mathcal{G}(\kappa), \mathcal{X}(\kappa), \mathcal{I}(\kappa)) \\ &\quad + \frac{\lambda}{\mathcal{M}(\lambda)\Gamma(\lambda)} \sum_{\xi=\gamma+1}^{\kappa} (\kappa - \rho(\xi))^{\lambda-1} \theta_2(\xi, \mathcal{G}(\xi), \mathcal{X}(\xi), \mathcal{I}(\xi)), \\ \mathcal{I}(\kappa) &= \mathcal{I}(\gamma) + \frac{1-\lambda}{\mathcal{M}(\lambda)}\theta_3(\kappa, \mathcal{G}(\kappa), \mathcal{X}(\kappa), \mathcal{I}(\kappa)) \\ &\quad + \frac{\lambda}{\mathcal{M}(\lambda)\Gamma(\lambda)} \sum_{\xi=\gamma+1}^{\kappa} (\kappa - \rho(\xi))^{\lambda-1} \theta_3(\xi, \mathcal{G}(\xi), \mathcal{X}(\xi), \mathcal{I}(\xi)). \end{aligned}$$

The following iterative scheme is formulated

$$\begin{aligned} \mathcal{G}_n(\kappa) &= \mathcal{G}_n(\gamma) + \frac{1-\lambda}{\mathcal{M}(\lambda)}\theta_1(\kappa, \mathcal{G}_{n-1}(\kappa), \mathcal{X}_{n-1}(\kappa), \mathcal{I}_{n-1}(\kappa)) \\ &\quad + \frac{\lambda}{\mathcal{M}(\lambda)\Gamma(\lambda)} \sum_{\xi=\gamma+1}^{\kappa} (\kappa - \rho(\xi))^{\lambda-1} \\ &\quad \times \theta_1(\xi, \mathcal{G}_{n-1}(\xi), \mathcal{I}_{n-1}(\xi), \mathcal{I}_{n-1}(\xi)), \end{aligned} \tag{17}$$

$$\begin{aligned} \mathcal{X}_n(\kappa) &= \mathcal{X}_n(\gamma) + \frac{1-\lambda}{\mathcal{M}(\lambda)}\theta_2(\kappa, \mathcal{G}_{n-1}(\kappa), \mathcal{X}_{n-1}(\kappa), \mathcal{I}_{n-1}(\kappa)) \\ &\quad + \frac{\lambda}{\mathcal{M}(\lambda)\Gamma(\lambda)} \sum_{\xi=\gamma+1}^{\kappa} (\kappa - \rho(\xi))^{\lambda-1} \\ &\quad \times \theta_2(\xi, \mathcal{G}_{n-1}(\xi), \mathcal{I}_{n-1}(\xi), \mathcal{I}_{n-1}(\xi)), \end{aligned} \tag{18}$$

$$\begin{aligned} \mathcal{I}_n(\kappa) &= \mathcal{I}_n(\gamma) + \frac{1-\lambda}{\mathcal{M}(\lambda)}\theta_3(\kappa, \mathcal{G}_{n-1}(\kappa), \mathcal{X}_{n-1}(\kappa), \mathcal{I}_{n-1}(\kappa)) \\ &\quad + \frac{\lambda}{\mathcal{M}(\lambda)\Gamma(\lambda)} \sum_{\xi=\gamma+1}^{\kappa} (\kappa - \rho(\xi))^{\lambda-1} \\ &\quad \times \theta_3(\xi, \mathcal{G}_{n-1}(\xi), \mathcal{I}_{n-1}(\xi), \mathcal{I}_{n-1}(\xi)). \end{aligned} \tag{19}$$

The exact solution of the problem can be determined as follows if the iteration system is established for terms bigger than  $n$  :

$$\begin{aligned} \mathcal{G}(\kappa) &= \lim_{n \rightarrow \infty} \mathcal{G}_n(\kappa), \\ \mathcal{X}(\kappa) &= \lim_{n \rightarrow \infty} \mathcal{X}_n(\kappa), \\ \mathcal{I}(\kappa) &= \lim_{n \rightarrow \infty} \mathcal{I}_n(\kappa). \end{aligned}$$

Thus, we get the required solution.

3. Results and discussion

The numerical results and discussion for the approximate solution for the considered model are provided in this section. To obtain the effect of the Nabla discrete ABC fractional derivative on the approximation solution (17)–(19) of the model (3). For the model we choose some suitable values for where the normal person and type-1 diabetes

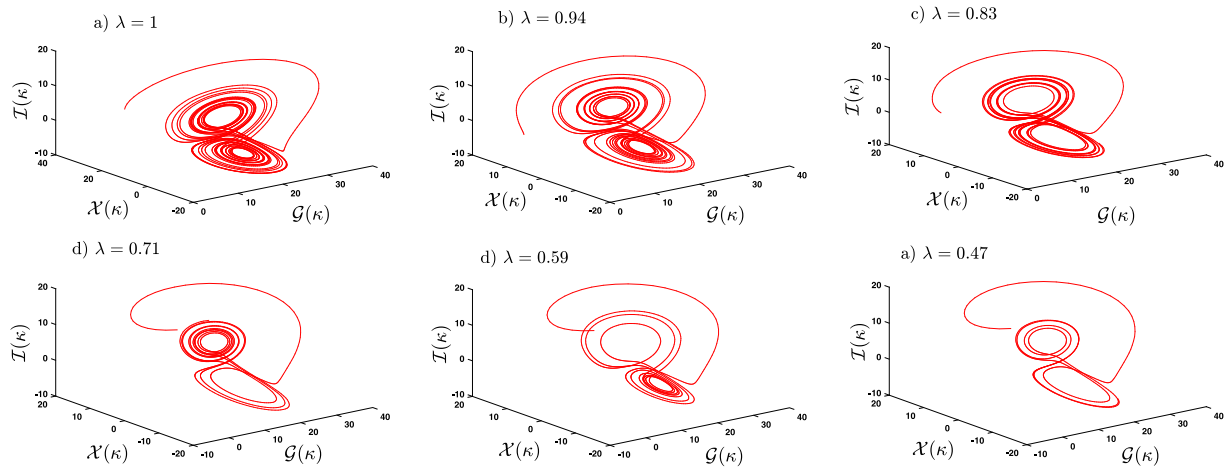


Fig. 5. Different differential order of the visualization of chaotic attractor of system (3) by trajectory with initial condition of  $G(0) = 0.83$ ,  $X(0) = 1.83$ ,  $I(0) = 1.03$  for the parameters given in Table 1.

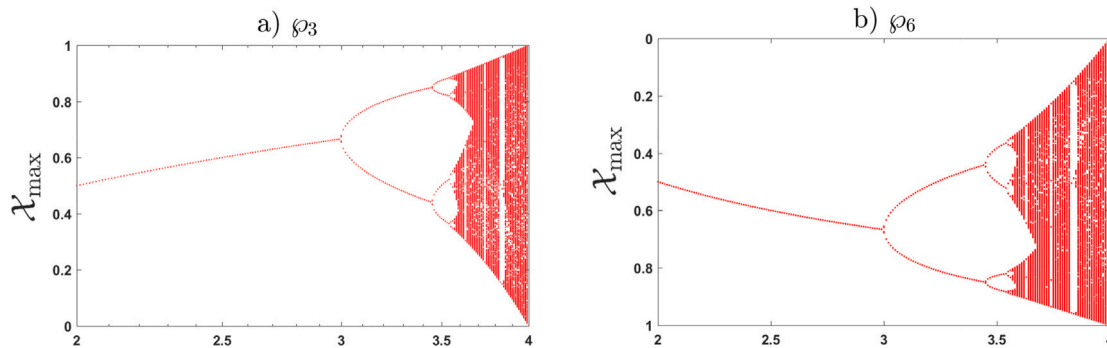


Fig. 6. The system (3) bifurcation diagram based on different values of parameters  $\varphi_3$  and  $\varphi_6$ .

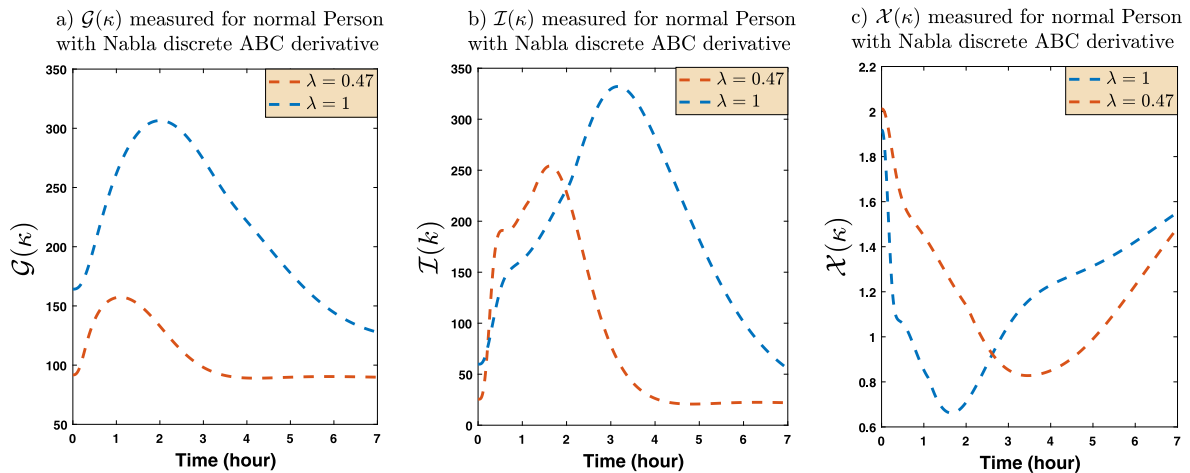


Fig. 7. Concentration profile for normal person with Nabla discrete fractional derivative of (a)  $G(\kappa)$ , (b)  $I(\kappa)$ , (c)  $X(\kappa)$ .

parameters value as shown in Table 1. The model dynamics are affected by a change in the value, according to these simulations.

First, we can obtain chaotic dynamics by varying the parameters; here, we focus on the varied dynamical behavior induced by different differential order  $\lambda$  as illustrated in Fig. 5. Following that, bifurcation

diagrams of the model (3) for various parameters are shown, and the biological significance of these diagrams is addressed. The quantities obtained or approaching stability by a system (chaotic attractors or periodic orbits, fixed points) are displayed against a bifurcation variable in the system in a bifurcation diagram. According to past research, if

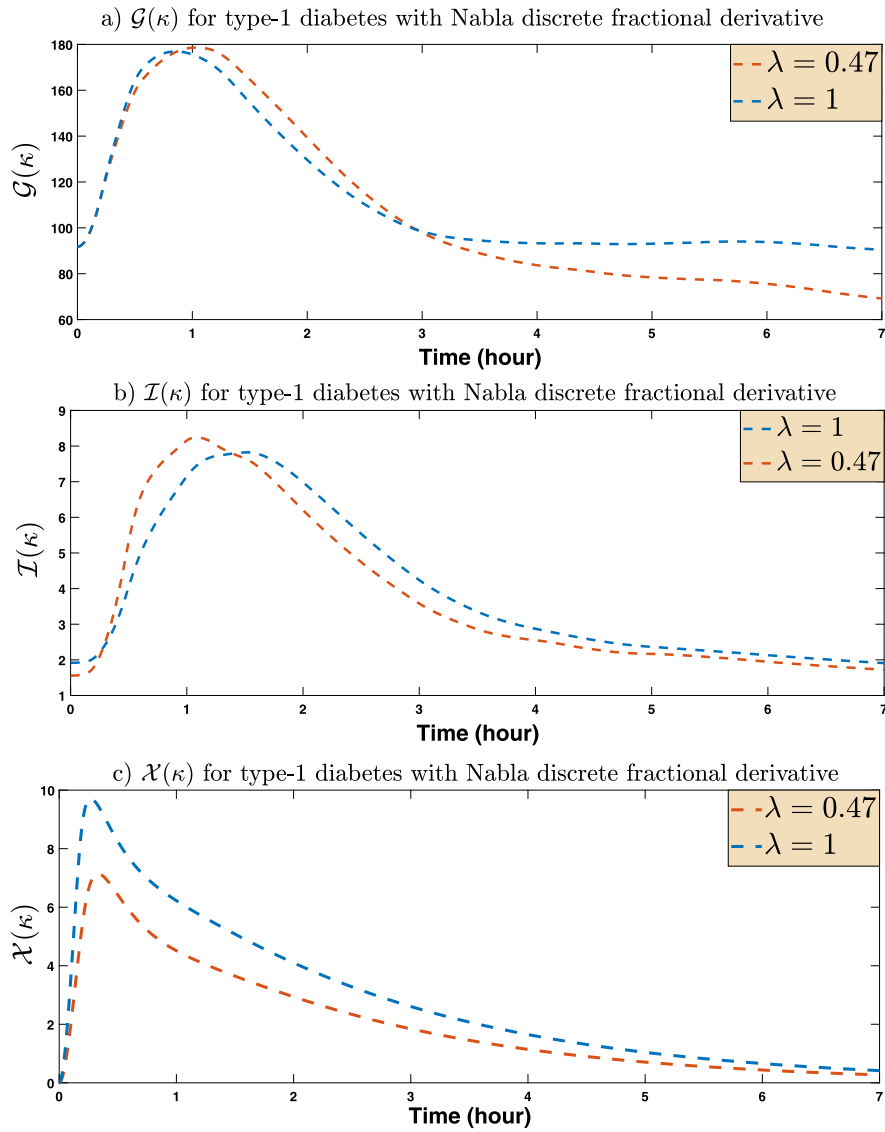


Fig. 8. Concentration profile for type-1 diabetes with Nabla discrete fractional derivative of (a)  $\mathcal{G}(\kappa)$ , (b)  $\mathcal{I}(\kappa)$ , (c)  $\mathcal{X}(\kappa)$ .

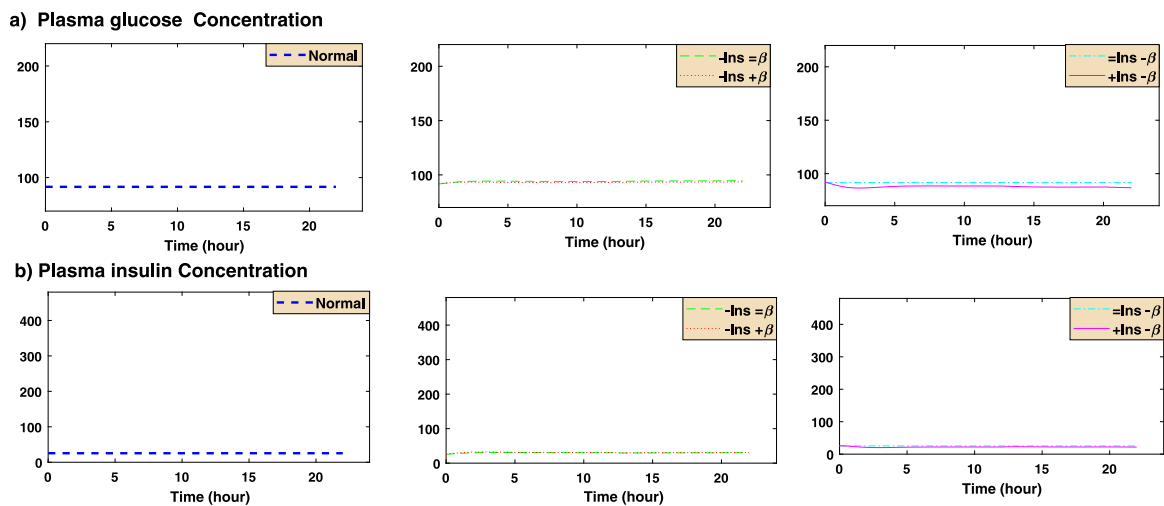


Fig. 9. Compare the plasma glucose and plasma insulin results.

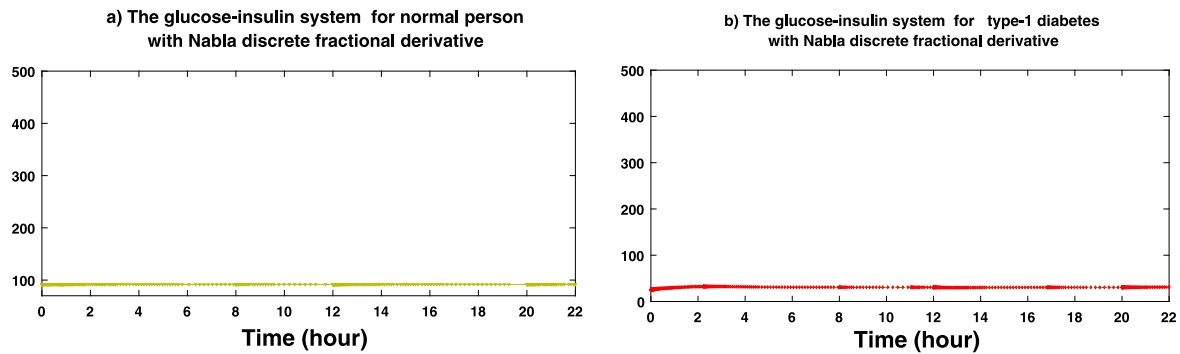


Fig. 10. The glucose–insulin system for a normal person as well as for type 1 diabetes mellitus.

Table 1

Parameters of normal person and type-1 diabetes in the model (see [40]).

Parameter	Normal person	Type-1 diabetes
$G_b$	80	80
$I_b$	7	15
$\varphi_1$	0.0317	0
$\varphi_2$	0.0123	0.017
$\varphi_3$	$4.92 \times 10^{-6}$	$5.3 \times 10^{-6}$
$\varphi_4$	0.0039	0.0042
$\varphi_5$	79.053	80.25
$\varphi_6$	0.2659	0.264

a system exhibits chaotic behavior, it indicates the presence of various disorder [8]. In the present work, whenever system acts chaotically we specify it as some kind of disorder. The suggested mathematical model simulates common GIRS-related disorders. Fig. 6 depicts the model of bifurcation diagram for various values of  $\varphi_3$  and  $\varphi_6$ . The local maxima of the time series ( $\mathcal{X}_{\max}$ ) are plotted for a few thousand iterations before the system is given time to settle down in order to depict the bifurcation diagrams of the system for each value of the control parameter. The system is stable for large values of parameters  $\varphi_3$  and  $\varphi_6$  but as these values (3.54 to 4) are increased, the system exhibits chaotic behavior.

Figs. 7–9 demonstrate the bounded solution for a normal person and type-1 diabetes based on normal glucose, insulin basal level, and insulin in plasma concentration. It should be noted that either low insulin sensitivity (low  $\beta$ -cell) or ( $-Ins = \beta$ , dashed green line), sensitivity ( $= Ins - \beta$ , dashed-dotted cyan line) lead to increased and prolonged plasma glucose concentrations (top row of plots). High sensitivity in another system can somewhat make up for low sensitivity in one system. For example, low insulin sensitivity and high  $\beta$ -cell sensitivity ( $-Ins + \beta$ , dotted red line) results in relatively normal plasma glucose concentrations (top row of plots). In this scenario, however, the resulting plasma insulin levels is exceedingly high (bottom row of plots). Fig. 10 depicts the entire behavior of the glucose–insulin system in both normal and type-1 diabetes. The graphical representations illustrate that the model is very dependent on the fractional-order  $\lambda$  and the model parameters chosen. We see that the classical system (i.e.  $\lambda = 1$ ) fails to stable the GIRS for both normal and type-1 DM, and does not maintain the close-loop design for an AP, for the GIRS presented in Figs. 8 and 9. Fig. 11 depicts a comparison of the GIRS Nabla ABC fractional derivative and the Nabla Caputo fractional derivative for a normal person and type-1 diabetes in each compartment. Therefore, the mathematical formulation established by the Nabla ABC fractional difference operator is useful in the simulation results indicates the actual and control situation of discrete monitoring of GIRS for the development of AP.

We discovered that when the derivative order  $\lambda$  is decreased from 1, the systems memory effect increases, causing the infection to spread slowly and the population of type-1 diabetics to grow for a long time. Because fractional derivatives have a memory property, the derivative

order  $\lambda$  influences the dynamics that describe patients with type-1 diabetes. When  $\lambda$  tends to 0, we find that the maximum levels of infection are reduced. The memory effect characterized by fractional derivative is reduced when  $\lambda$  limits to 1. Therefore, by reducing the memory effect, the maximum levels of the infection are reduced. Furthermore, the results demonstrated that the fractional-order model provides better insight into the effect of treatment on type-1 diabetes than the classical model with integer-order derivatives. On the other hand, by taking into consideration mathematical models on time scales, i.e. dynamic models can be used to find solutions to corresponding continuous and discrete models. This helps to avoid solving models individually on their own domain. This has been demonstrated to be significant when analyzing the type-1 DM dynamics model. It is also worth noting that a mathematical model on time scales can provide not only continuous model, but a discrete models as well.

#### 4. Conclusion

In this paper, the new models of GIRS on DMs to the concept of Nabla discrete ABC fractional derivative operator and AB fractional integral operator are introduced. The model implementation is based on the ABC derivative and discretization while using the nabla fractional-order difference. Note that, the memory effect and the non-singular kernel constitute two properties that characterize the Nabla discrete ABC fractional derivative and explain its emergence these last years in modeling biological phenomena. We study the impact of fractional orders of the model derivatives on the dynamic properties of the proposed model. The existence and uniqueness of solution of the Nabla discrete ABC fractional diabetes model is established by using the Banach fixed point theorem approach. We obtain the approximate solution of the models and a numerical solution of the models which shows that effect of time on the concentrations  $G(\kappa)$ ,  $I(\kappa)$ ,  $\mathcal{X}(\kappa)$  and also the difference between a normal person and diabetic person is shown in the GIRS. The model provide the continues glucose measuring in limited time and solutions are bounded in normal values for healthy person and type-1 diabetes. The results are very useful to design the AP to overcome the risk of hyperglycemia.

We hope this work will help the some researchers work in further new direction of applied mathematics:

(1) Many countries are now seeing an increase in the spread of the COVID-19 pandemic, which has major economic, social, and health implications. We propose a Nabla discrete ABC fractional difference operator mathematical model for the dynamics of how COVID-19 disease spreads, as well as a mathematical model for the dynamics of diabetes, and then highlight the harmful effect quarantine has on diabetic health [54].

(2) The practical implementation of the controller employing AP (see [2,3]), as well as further development of the discrete-time control method to address the problem of glucose–insulin hemostat using bi-hormonal insulin and glucagon synthesis.

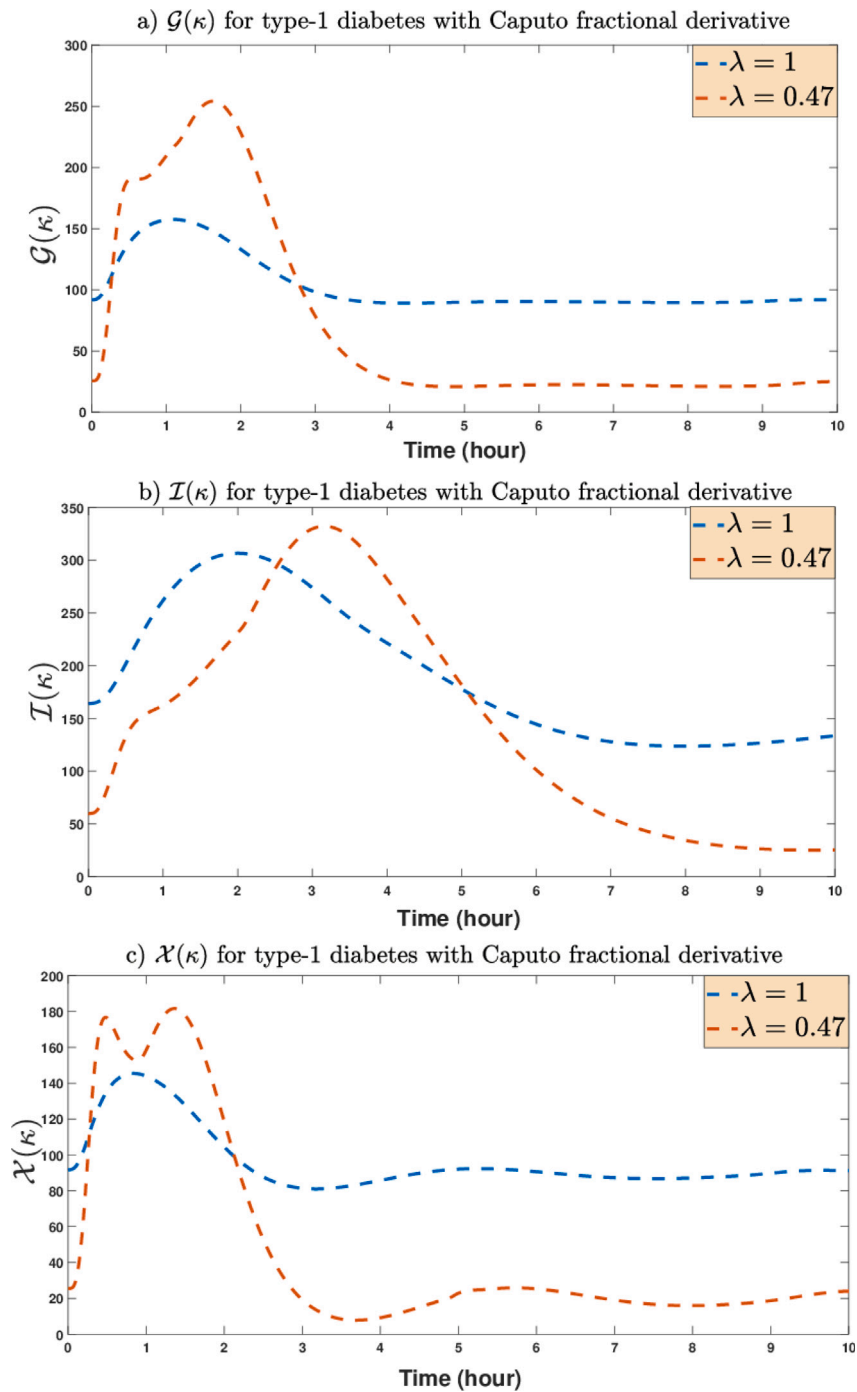


Fig. 11. The glucose–insulin system for a normal person as well as for type 1 diabetes mellitus.

**CRedit authorship contribution statement**

**G. Narayanan:** Conceptualization, Methodology, Software. **M. Syed Ali:** Supervision. **Grienggrai Rajchakit:** Data curation, Writing – original draft. **Anuwat Jirawattanapanit:** Visualization, Investigation. **Bandana Priya:** Software, Validation.

**Declaration of competing interest**

The authors declare that they have no known competing financial interests or personal relationships that could have appeared to influence the work reported in this paper.

**Data availability**

No data was used for the research described in the article.

**Acknowledgments**

The authors thanks the financial support from National Research Council of Thailand (Talented Mid-Career Researchers) Grant Number N42A650250.

### Ethics approval and consent to participate

This article does not contain any studies with human participants or animals performed by any of the authors. This article does not include human participants.

### References

- [1] H.M. Srivastava, R.S. Dubey, M. Jain, A study of the fractional-order mathematical model of diabetes and its resulting complications, *Math. Methods Appl. Sci.* 42 (2019) 4570–4583.
- [2] S.Z. Birjandi, S.K.H. Sani, N. Pariz, Insulin infusion rate control in type 1 diabetes patients using information-theoretic model predictive control, *Biomed. Signal Process. Control* 76 (2022) 103635.
- [3] F. Rahmani, M. Dehghani, P. Karimaghaee, M. Mohammadi, R. Abolpour, Hardware-in-the-loop control of glucose in diabetic patients based on nonlinear time-varying blood glucose model, *Biomed. Signal Process. Control* 66 (2021) 102467.
- [4] I. Ahmad, F. Munir, M.F. Munir, An adaptive backstepping based non-linear controller for artificial pancreas in type 1 diabetes patients, *Biomed. Signal Process. Control* 47 (2019) 49–56.
- [5] P.S. Shabestari, S. Panahi, B. Hatef, S. Jafari, J.C. Sprott, A new chaotic model for glucose-insulin regulatory system, *Chaos Solitons Fractals* 112 (2018) 44–51.
- [6] M. Farman, M.U. Saleem, M.O. Ahmed, A. Ahmad, Stability analysis and control of the glucose insulin glucagon system in humans, *Chinese J. Phys.* 56 (2018) 1362–1369.
- [7] A. Makroglou, J. Li, Y. Kuang, Mathematical models and software tools for the glucose-insulin regulatory system and diabetes: an overview, *Appl. Numer. Math.* 56 (2006) 559–573.
- [8] A.A. Hussein, F. Rahma, S. Jafari, Hopf bifurcation and chaos in time-delay model of glucose-insulin regulatory system, *Chaos Solitons Fractals* 137 (2020) 109845.
- [9] M. Farman, M.U. Saleem, M.F. Tabassum, A. Ahmad, M.O. Ahmad, A linear control of composite model for glucose insulin glucagon pump, *Ain Shams Eng. J.* 10 (2019) 867–872.
- [10] G. Quiroz, R. Femat, On hyperglycemic glucose basal levels in Type 1 Diabetes Mellitus from dynamic analysis, *Math. Biosci.* 210 (2007) 554–575.
- [11] H. Wang, J. Li, Y. Kuang, Mathematical modeling and qualitative analysis of insulin therapies, *Math. Biosci.* 210 (2007) 17–33.
- [12] A. Mahata, S.P. Mondal, S. Alam, B. Roy, Mathematical model of glucose-insulin regulatory system on diabetes mellitus in fuzzy and crisp environment, *Ecol. Genet. Genom.* 2 (2017) 25–34.
- [13] K. Han, H. Kang, M.Y. Choi, J. Kim, M.S. Lee, Mathematical model of the glucose-insulin regulatory system: From the bursting electrical activity in pancreatic  $\beta$ -cells to the glucose dynamics in the whole body, *Phys. Lett. A* 376 (2012) 3150–3157.
- [14] J. Yang, S. Tang, R.A. Cheke, The regulatory system for diabetes mellitus: Modeling rates of glucose infusions and insulin injections, *Commun. Nonlinear Sci. Numer. Simul.* 37 (2016) 305–325.
- [15] Q. Zhu, Stability analysis of stochastic delay differential equations with Levy noise, *Systems Control Lett.* 118 (2018) 62–68.
- [16] Q. Zhu, Razumikhin-type theorem for stochastic functional differential equations with Levy noise and Markov switching, *Internat. J. Control* 90 (2017) 1703–1712.
- [17] X. Li, X. Yang, J. Cao, Event-triggered impulsive control for nonlinear delay systems, *Automatica* 117 (2020) 108981.
- [18] O.M. Kwon, S.H. Lee, M.J. Park, Some novel results on stability analysis of generalized neural networks with time-varying delays via augmented approach, *IEEE Trans. Cybern.* 52 (2022) 2238–2248.
- [19] X. Li, X. Yang, S. Song, Lyapunov conditions for finite-time stability of time-varying time-delay systems, *Automatica* 103 (2019) 135–140.
- [20] O.M. Kwon, S.H. Lee, M.J. Park, S.M. Lee, Augmented zero equality approach to stability for linear systems with time-varying delay, *Appl. Math. Comput.* 381 (2020) 125329.
- [21] E. Arslan, G. Narayanan, M. Syed Ali, S. Arik, S. Saroha, Controller design for finite-time and fixed-time stabilization of fractional-order memristive complex-valued BAM neural networks with uncertain parameters and time-varying delays, *Neural Netw.* 130 (2020) 60–74.
- [22] P. Balasubramaniam, P. Muthukumar, K. Ratnavelu, Theoretical and practical applications of fuzzy fractional integral sliding mode control for fractional-order dynamical system, *Nonlinear Dynam.* 80 (2015) 249–267.
- [23] P. Muthukumar, P. Balasubramaniam, K. Ratnavelu, Sliding mode control for generalized robust synchronization of mismatched fractional order dynamical systems and its application to secure transmission of voice messages, *ISA Trans.* 82 (2018) 51–61.
- [24] K. Hattaf, On the stability and numerical scheme of fractional differential equations with application to biology, *Computation* 10 (2022) 97.
- [25] J. Cao, G. Stamov, I. Stamova, S. Simeonov, Almost periodicity in impulsive fractional-order reaction–diffusion neural networks with time-varying delays, *IEEE Trans. Cybern.* 51 (2021) 151–161.
- [26] C. Huang, J. Cao, Bifurcation mechanism of a fractional-order neural network with unequal delays, *Neural Process. Lett.* 52 (2020) 1171–1187.
- [27] K. Hattaf, A new generalized definition of fractional derivative with non-singular kernel, *Computation* 8 (2020) 49.
- [28] M. Syed Ali, G. Narayanan, V. Shekher, A. Alsaedi, B. Ahmad, Global Mittag-Leffler stability analysis of impulsive fractional-order complex-valued BAM neural networks with time varying delays, *Commun. Nonlinear Sci. Numer. Simul.* 83 (2020) 105088.
- [29] M. Syed Ali, G. Narayanan, V. Shekher, H. Alsulami, T. Saeed, Dynamic stability analysis of stochastic fractional-order memristor fuzzy BAM neural networks with delay and leakage terms, *Appl. Math. Comput.* 369 (2020) 124896.
- [30] H. Khan, J.F. Gomez-Aguilar, A. Alkhazzan, A. Khan, A fractional-order HIV-TB coinfection model with nonsingular Mittag-Leffler Law, *Math. Methods Appl. Sci.* 43 (2020) 3786–3806.
- [31] G. Nazir, K. Shah, A. Debbouche, R.A. Khan, Study of HIV mathematical model under nonsingular kernel type derivative of fractional order, *Chaos Solitons Fractals* 139 (2020) 110095.
- [32] N. Sene, SIR epidemic model with Mittag-Leffler fractional derivative, *Chaos Solitons Fractals* 137 (2020) 109833.
- [33] P.A. Naik, K.M. Owolabi, M. Yavuz, J. Zu, Chaotic dynamics of a fractional order HIV-1 model involving AIDS-related cancer cells, *Chaos Solitons Fractals* 140 (2020) 110272.
- [34] A. Khan, J.F. Gomez-Aguilar, T.S. Khan, H. Khan, Stability analysis and numerical solutions of fractional order HIV/AIDS model, *Chaos Solitons Fractals* 122 (2019) 119–128.
- [35] A.N. Chatterjee, B. Ahmad, A fractional-order differential equation model of COVID-19 infection of epithelial cells, *Chaos Solitons Fractals* 147 (2021) 110952.
- [36] I.A. Baba, B. Ahmad, Fractional order epidemic model for the dynamics of novel COVID-19, *Alex. Eng. J.* 60 (2021) 537–548.
- [37] M. Sher, K. Shah, Z.A. Khan, H. Khan, A. Khan, Computational and theoretical modeling of the transmission dynamics of novel COVID-19 under Mittag-Leffler Power Law, *Alex. Eng. J.* 59 (2020) 3133–3147.
- [38] V. Padmavathi, A. Prakash, K. Alagesan, N. Magesh, Analysis and numerical simulation of novel coronavirus (COVID-19) model with Mittag-Leffler Kernel, *Math. Methods Appl. Sci.* 44 (2021) 1863–1877.
- [39] J. Singh, D. Kumar, D. Baleanu, On the analysis of fractional diabetes model with exponential law, *Adv. Difference Equ.* 231 (2018) <http://dx.doi.org/10.1186/s13662-018-1680-1>.
- [40] M.U. Saleem, M. Farman, A. Ahmad, E. Haque, M.O. Ahmad, A Caputo Fabrizio fractional order model for control of glucose in insulin therapies for diabetes, *Ain Shams Eng. J.* 11 (2020) 1309–1316.
- [41] M. Farman, M.U. Saleem, A. Ahmad, S. Imtiaz, M.F. Tabassum, S. Akram, M.O. Ahmad, A control of glucose level in insulin therapies for the development of artificial pancreas by Atangana Baleanu derivative, *Alex. Eng. J.* 59 (2020) 2639–2648.
- [42] T. Abdeljawad, On Riemann and Caputo fractional differences, *Comput. Math. Appl.* 62 (2011) 1602–1611.
- [43] T. Abdeljawad, Dual identities in fractional difference calculus within Riemann, *Adv. Difference Equ.* 36 (2013) <http://dx.doi.org/10.1186/1687-1847-2013-36>.
- [44] T. Abdeljawad, On delta and nabla Caputo fractional differences and dual identities, *Discrete Dyn. Nat. Soc.* 2013 (2013) 406910.
- [45] A. Khan, H.M. Alshehri, T. Abdeljawad, Q.M. Al-Mdallal, H. Khan, Stability analysis of fractional nabla difference COVID-19 model, *Results Phys.* 22 (2021) 103888.
- [46] L. Chen, H. Yin, T. Huang, L. Yuan, S. Zheng, L. Yin, Chaos in fractional-order discrete neural networks with application to image encryption, *Neural Netw.* 125 (2020) 174–184.
- [47] M.T. Holm, The Laplace transform in discrete fractional calculus, *Comput. Math. Appl.* 62 (2011) 1591–1601.
- [48] D. Baleanu, G.C. Wu, Y.R. Bai, F.L. Chen, Stability analysis of Caputo-like discrete fractional systems, *Commun. Nonlinear Sci. Numer. Simul.* 48 (2017) 520–530.
- [49] Y. Wei, Y. Wei, Y. Chen, Y. Wang, Mittag-Leffler stability of nabla discrete fractional-order dynamic systems, *Nonlinear Dynam.* 101 (2020) 407–417.
- [50] T. Abdeljawad, D. Baleanu, Discrete fractional differences with nonsingular discrete Mittag-Leffler kernels, *Adv. Difference Equ.* 232 (2016) <http://dx.doi.org/10.1186/s13662-016-0949-5>.
- [51] T. Abdeljawad, Fractional difference operators with discrete generalized Mittag-Leffler kernels, *Chaos Solitons Fractals* 126 (2019) 315–324.

- [52] T. Abdeljawad, Q.M. Al-Mdallal, Discrete Mittag-Leffler kernel type fractional difference initial value problems and Grönwall's inequality, *J. Comput. Appl. Math.* 339 (2018) 218–230.
- [53] T. Abdeljawad, D. Baleanu, Monotonicity analysis of a nabla discrete fractional operator with discrete Mittag-Leffler kernel, *Chaos Solitons Fractals* 102 (2017) 106–110.
- [54] A. Koudere, L.E. Youssoufi, H. Ferjouchia, O. Balatif, M. Rachik, Optimal control of mathematical modeling of the spread of the COVID-19 pandemic with highlighting the negative impact of quarantine on diabetics people with cost-effectiveness, *Chaos Solitons Fractals* 145 (2021) 110777.